NGL-05-002-127

PHOTOELECTRIC SPECTROPHOTOMETRY OF OQ 172 AND OH 471

by

J. B. Oke

Hale Observatories, California Institute of Technology

Carnegie Institution of Washington

Received: _____

Send proofs to:
J. B. Oke
Hale Observatories
California Institute of Technology 105-24
Pasadena, Ca. 91109

ABSTRACT

Absolute spectral energy distributions for the large redshift quasars OQ 172 and OH 471 are discussed along with similar data for two other quasars 4C05.34 and PHL 957. Assuming cosmological redshifts, OQ 172 and OH 471 are not as luminous as PHL 957. If these quasars are basically similar and if radiative processes dominate, the strength of Ly α and the behavior of the continuum at the Lyman limit strongly suggest that these objects consist of a central ionizing source surrounded by discrete clouds, filaments or a gaseous structure such as a disk. This gaseous matter does not cover the whole solid angle surrounding the source.

Subject Headings: Quasi-stellar sources - Spectrophotometry

INTRODUCTION

The discovery that the two radio sources OQ 172 and OH 471 have redshifts respectively of 3.53 and 3.40 provides for the first time an excellent opportunity to look in detail at the continuum spectrum above and below the Lyman limit. In the case of OH 471, Carswell and Strittmatter (1973) identified two emission lines with Lα and with O VI (λλ1031.9, 1037.6) or Lβ (λ1026). The emission line redshift of OQ 172 (Wampler et al 1973) depends on the identification of Lα and λ1550 of C IV. There is also some evidence for a feature at Lβ or O VI. Both objects have rich absorption-line spectra.

OBSERVATIONS

Absolute spectral energy distributions for OQ 172 and OH 471 were obtained with the multichannel spectrometer attached to the 200-inch (508 cm) Hale telescope. The results are shown in Figure 1 where log f_ν is plotted against the observed log ν for both objects. The flux f_ν is in units of ergs sec^{-1} cm^{-2} Hz^{-1}; the energy distributions are based on the absolute calibration of α Lyrae as given by Oke and Schild (1970). For each energy distribution, the locations of the Lyman limit L_L, Lβ or O VI, Lα, λ1550 of C IV, and λ1909 of CIII] are marked. In both objects the CIII] line, which was not used in determining the published redshift, is clearly present at the correct position. In both objects

there is a line at the position of Lβ or OVI.

RESULTS

In discussing results for these two objects we will also discuss similar data which is available for two other large redshift objects 4C05.34 (Oke 1970, Lynds 1971) and PHL 957 (Lowrance et al 1972).

The continua of these four objects cannot really be represented adequately by a power law. The reason for this may be partly intrinsic but it is also a consequence of the many absorption lines below emission Lα which are not resolved by the multichannel spectrometer. Since a power law is adequate on the red side of Lα, we have tabulated the spectral index α, where $f_\nu \propto \nu^\alpha$, for this spectral range in Table 1. The mean value of α between the radio and optical regions is -0.7 for OQ 172, OH 471, and 4C05.34.

It is also useful to list the observed flux f_ν at the frequency corresponding to the redshifted frequency of 10^{15} Hz as has been done for many other quasars (Oke et al 1970). These fluxes require a modest extrapolation beyond the redmost frequencies observed. These are also listed in Table 1 for all four objects. The relationship between the emitted flux F_{ν_o} at the source at rest frequency ν_o and the observed flux f_ν measured at the redshifted frequency of ν_o is

$$F_{\nu_o} = 1.07 \times 10^{57} \left(\frac{100}{H_o}\right)^2 \frac{z^2}{1+z} f_\nu , \qquad (1)$$

where H_o is the Hubble constant in km sec^{-1} Mpc^{-1}. The above formula applies for $q_o = +1$. For $q_o = 0$, the right hand side of the equation is multiplied by $(1 + \frac{1}{2}z)^2$. Values of log F_{ν_o} are given in Table 1 for $\nu_o = 10^{15}$ Hz, $H_o = 100$ km sec^{-1} mpc^{-2}, and $q_o = +1$. They can be compared directly with similar data for other quasars (Oke et al 1970). (In Table 1 of the reference just mentioned, the values of log F_{ν_o} (10^{15} Hz) should be increased by 3 to give units of ergs sec^{-1} Hz^{-1}). The absolute luminosities of OQ 172 and OH 471 are comparable with that of 4C05.34 but less than that of PHL 957. Using models with $q_o = 0$ does not alter the relative luminosities of these four objects significantly.

The most striking difference between the energy distributions of OQ 172 and OH 471 is their behavior below the Lyman limit. In OQ 172 there is essentially no change at the limit, while in OH 471 there is a drop corresponding to a factor 5. In this latter object the smooth and gradual drop of intensity with wavelength near the Lyman limit is compatible with the breadths of the emission lines seen in the spectrum. In 4C05.34 the drop of intensity as one crosses the Lyman limit is about a factor 2, while in PHL 957, the redshift is too low to measure adequately the flux below the limit. The ratio of intensities $I(1216^+)/I(1216^-)$ is given in Table 1.

In Table 2 are given the intensities of the observed emission lines in terms of (1) equivalent width in Angstroms, (2) observed intensity j ergs $sec^{-1}cm^{-2}$, and (3) absolute emitted intensity J ergs sec^{-1}. The relation between j and J is

$$J = 1.07 \times 10^{57} \left(\frac{100}{H_o}\right)^2 z^2 j \qquad (2)$$

for $q_o = +1$. The right hand side is multiplied by $(1 + \frac{1}{2}z)^2$ for $q_o = 0$. J in Table 2 is based on $H_o = 100$ km sec^{-1} mpc^{-1} and $q_o = +1$. For Lα two sets of numbers are given in 3 cases. The first corresponds to the observed equivalent width. Lα, however, is asymmetrical, being depressed on the violet wing, presumably by absorption lines. The second sets of numbers correspond approximately to twice the equivalent width measured from the line center redwards. The range of equivalent width for each line is typically a factor 3, but over a factor 4 for λ1909 of C III].

DISCUSSION

We consider the observations first in terms of a model in which a small central source, which provides the ionizing radiation, is surrounded by a spherically symmetrical nebula of ionized low density gas. We further assume that processes are radiative, that the Lyman emission lines are produced by recombination, and that the Lyman photons degenerate into Lα

when multiple scattering occurs. If the nebula is optically thin to Lyman radiation, then for an electron temperature of 10,000 to 20,000 °K the ratio of intensities of Lα to Lβ is 4.0 (Bahcall 1966). As the optical depth increases this ratio increases. Although our data are not adequate to determine whether the emission feature near Lβ is due to Lβ or O VI, it still provides an upper limit to the strength of Lβ. In the case of OQ 172, the ratio of Lα to the Lβ feature is consistent with an optically thin nebula; if the Lβ feature is really O VI, then the nebula is optically thick. For OH 471 and 4C05.34, the ratio is at least 10 to 20 corresponding to optical depths in the center of Lβ of at least 3 (Bahcall 1966).

We can also make a direct comparison between the number of Lα photons observed and the number of Lyman continuum photons emitted by the central ionizing source, which do not escape from the nebula. This latter can be estimated by extrapolating the continuum between Lα and L_L to much higher frequencies and allowing for the radiation still seen below the Lyman limit. When this is done for OH 471 and 4C05.34, Lα has too few photons by factors of 2.2 and 1.7 respectively. For the proposed spherical model there are at least two possible explanations. (1) If the optical depth at the Lyman limit is moderate, as indeed appears to be the case for this model, the Lyman opacity rapidly decreases to practically zero at higher frequencies and Lyman photons are mostly

absorbed just below the Lyman limit. (2) The radiative flux from the central source may decrease rapidly at higher frequencies. A cut off at 700 Å [near log ν (obs) = 10^{15} in OH 471] would fit the observations.

A third possible solution is to postulate a model in which the nebula is not spherically symmetrical, but is in the form of clouds or some structure such as a thick disk, which does not cover the whole solid angle around the source. In this case the observed Lα intensity is produced by all the gas, and may correspond to an optically thin or optically thick case. The amount of radiation below the Lyman limit converted to Lα will depend on the fraction of the total solid angle about the source covered by clouds. The observed flux below the Lyman limit, on the other hand, will be governed by the amount of material in the line-of-sight to the central source; this may be large, small, or negligible. The observations of OH 471 and 4C05.34 do not distinguish among any of these models.

The observations of OQ 172 present an interesting and important difference from those of OH 471 and 4C05.34. Here Lα is observed with the usual equivalent width, but there is no discontinuity at the Lyman limit. In terms of the spherically symmetrical model, the strength of Lα requires a drop in intensity at the Lyman limit by 30 percent, which should occur just below the limit where the opacity is high. This is not observed. One could imagine an optically thin

gas with pure recombination, as is possible from the Lα/Lβ ratio, but such recombination produces not only Lα and Lβ but a Lyman continuum in emission with an intensity comparable with Lα itself. To produce the observed lines and no Lyman jump in this case requires a non-static model with just the right parameters, a rather unlikely situation. Thus a spherically symmetrical model does not work.

The observations of OQ 172 can however be explained with the third cloud or disk model. For this object the clouds or disk could be optically thin or optically thick while the Lyman absorption in the line-of-sight to the central source is very small.

Considering all three objects to be basically similar, the most reasonable model, if radiative processes dominate, is one in which the gas surrounding the central source is in clouds or in a restricted zone such as a disk, so that the gas subtends only a fraction of the total solid angle as seen from the central source. Such a model has been proposed by Schmidt (1964) to avoid the problem which electron scattering poses for highly variable quasars.

COLORS

The B-V colors of OQ 172 and OH 471 can be estimated roughly from the energy distributions and are approximately +0.6. The rather red color for a quasar is due to the presence of Lα in the V band. The U-B color will put OQ 172 above the black-body curve in the two color diagram and OH 471 below the domain usually occupied by unreddened stars. Therefore these objects can be found by suitable 2-color surveys. There will presumably be other quasars with Lyman jumps intermediate between those of OQ 172 and OH 471 which mimic normal star colors. At redshifts of about 4.4 objects like OQ 172 will remain near the black-body line in the 2-color diagram, and an object like OH 471 will become extremely red with B-V of the order of +1.5 to +2.0. It will still be possible to discover such objects with photographic surveys, although intermediate objects will be missed.

This work was supported in part by the National Aeronautics and Space Administration through grant NGL-05-002-134.

TABLE 1

Continuum Data

Object	z	log (f_ν) (ergs $sec^{-1}cm^{-2}Hz^{-1}$)	log F_{ν_o} (10^{15}Hz) (ergs $sec^{-1}Hz^{-1}$)	α (above Lα)	$\frac{I(1216^+)}{I(1216^-)}$
OQ 172	3.53	-26.38	31.09	-0.5	1
OH 471	3.40	-26.52	30.93	-1.1	5
4C05.34	2.877	-26.44	30.92	-0.8	2
PHL 957	2.69	-25.96	31.36	-0.3	?

TABLE 2

Emission Line Data*

Object	C III], λ1909			C IV, λ1550			Lα, λ1216			Lβ or O VI		
	W	$jx10^{15}$	$Jx10^{-42}$	W	$jx10^{15}$	$Jx10^{-42}$	W	$jx10^{15}$	$Jx10^{-42}$	W	$jx10^{15}$	$Jx10^{-42}$
OQ 172	229	29.0	387	61	11.2	149	249	59.0	786	67	16.1	215
							352†	83.5	1113			
OH 471	152	10.2	126	101	9.4	116	400	38.2	472	27	2.8	34
							560†	53.6	662			
4C05.34	50	7.0	62	147	26.0	230	462	97.0	860	40	8.5	75
PHL 957	66	37.0	289	56	45.0	349	129	150.0	1170	-	-	-
							152†	177.0	1380			

* W is equivalent width in A, j is observed intensity in ergs $sec^{-1}cm^{-2}$, and J is emitted intensity in ergs sec^{-1}.

† Twice the equivalent width from the line center redwards.

REFERENCES

Bahcall, J.N. 1966, Ap. J., 145, 684.

Carswell, R.F. and Strittmatter, P.A. 1973, Nature, 242, 394.

Lowrance, J.L., Morton, D.C., Zucchino, P., Oke, J.B., and Schmidt, M. 1972, Ap.J., 171, 233.

Lynds, R. 1971, Ap. J. (Letters), 164, L73.

Oke, J.B., Neugebauer, G., and Becklin, E.E. 1970, Ap.J., 159, 341.

Oke, J.B. and Schild, R.E. 1970, Ap.J., 161, 1015.

Oke, J.B. 1970, Ap.J. (Letters), 161, L17.

Schmidt, M. 1964, Quasars and High-Energy Astronomy (New York: Gordon and Breach 1969) p. 55.

Wampler, E.J., Robinson, L.B., Baldwin, J.A., and Burbidge, E.M. 1973, Nature, 243, 336.

CAPTIONS

Fig. 1 Absolute spectral energy distributions for OQ 172 and OH 471. Log f_ν , where f_ν is the flux in ergs $sec^{-1}cm^{-2}Hz^{-1}$ is plotted against log ν where ν is the observed frequency. The positions of several emission lines and the Lyman limit L_L are indicated. "At" marks the region of strong atmospheric water-vapor absorption. Standard deviation bars are included if they are significantly larger than the dots themselves.

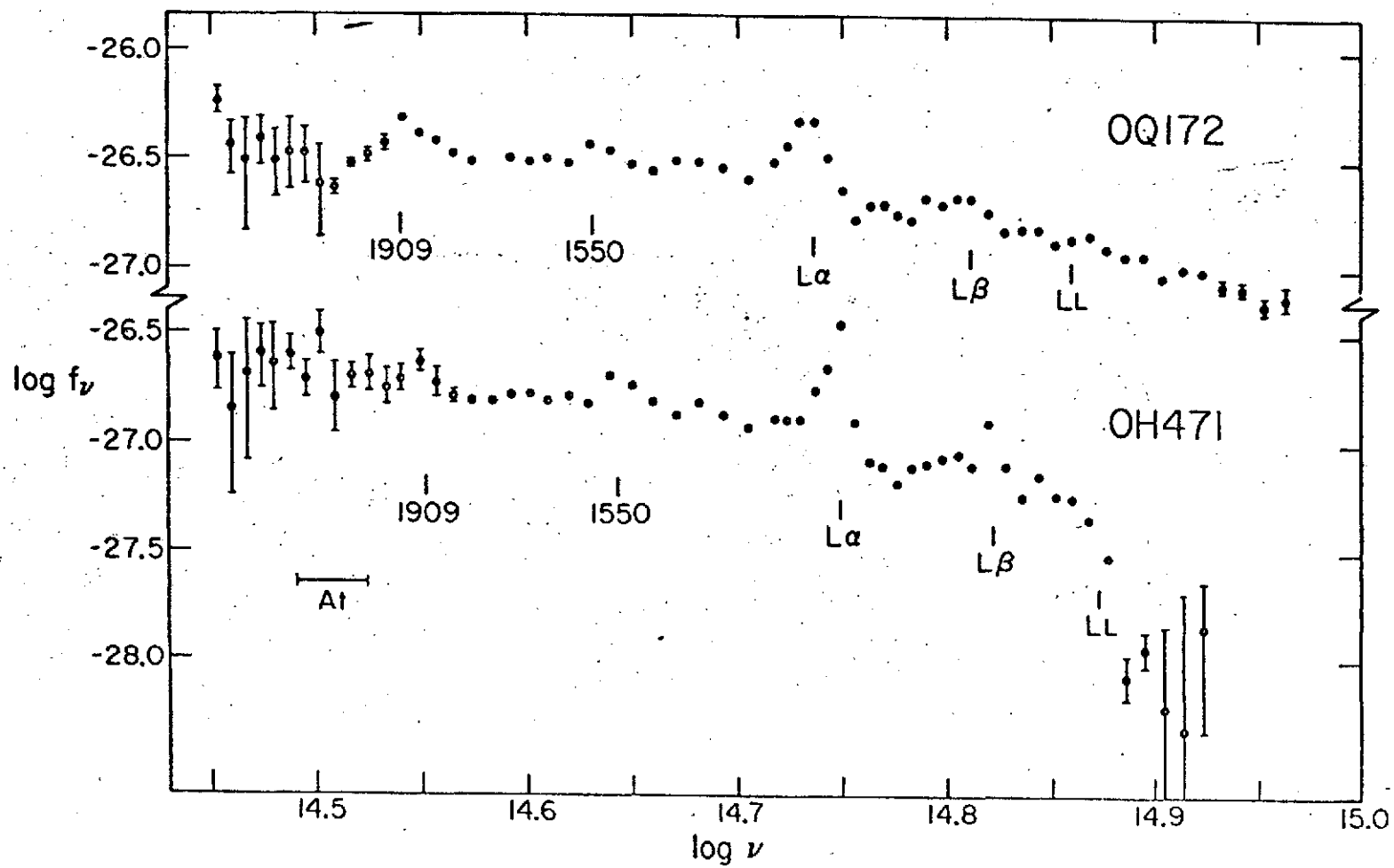
-26.0
-26.5
-27.0
-26.5
-27.0
-27.5
-28.0
log f_ν
OQ172
1909
1550
Lα
Lβ
LL
OH471
1909
1550
Lα
Lβ
LL
At
14.5
14.6
14.7
14.8
14.9
15.0
log ν

Oke Fig. 1.